MOLECULAR AND CELLULAR BIOLOGY, Jan. 1997, p. 209–218 Vol. 17, No. 1
0270-7306/97/$04.00+0


# Postfertilization Deadenylation of mRNAs in *Xenopus laevis* Embryos Is Sufficient To Cause Their Degradation at the Blastula Stage

YANN AUDIC, FRANCIS OMILLI, AND H. BEVERLEY OSBORNE*

*Centre National de la Recherche Scientifique, UPR 41, Université de Rennes I, Campus de Beaulieu, 35042 Rennes Cédex, France*

Received 30 May 1996/Returned for modification 6 August 1996/Accepted 4 October 1996

**Although the maternal *Xenopus laevis* Eg mRNAs are deadenylated after fertilization, they are not immediately degraded and they persist in the embryos as poly(A)$^-$ transcripts. The degradation of these RNAs is not detected until the blastula stage of development (6 to 7 h postfertilization). To understand the basis for this delay between deadenylation and degradation, it is necessary to identify the *cis*-acting element(s) required to trigger degradation in blastula stage embryos. To this end, several chimeric RNAs containing different portions of the 3′ untranslated region of Eg2 mRNA were injected into two-cell *X. laevis* embryos. We observed that only the RNAs that contained the *cis*-acting elements that confer rapid deadenylation were subsequently degraded at the blastula stage. This suggested that deadenylation may be sufficient to trigger degradation. By injecting chimeric RNAs devoid of Eg sequence information, we further showed that only deadenylated RNAs were degraded in *X. laevis* embryos. Last, introduction of a functional cytoplasmic polyadenylation element into a poly(A)$^-$ RNA, thereby causing its polyadenylation after injection into embryos, protected the RNA from degradation. Hence, in *X. laevis* embryos, the postfertilization deadenylation of maternal Eg mRNAs is sufficient to cause the degradation of an mRNA, which, however, only becomes apparent at the blastula stage. Possible causes for this delay between deadenylation and degradation are discussed in the light of these results.**

In many species, transcription is effectively silent during the period encompassing the meiotic maturation and the early development that immediately follows fertilization. From this it follows that the regulation of gene expression at the post-transcriptional level (localization, translation and stability) probably plays a critical role in the control of early development. In *Drosophila melanogaster* the importance of controlling the localization and the translation of specific maternal mRNAs has been clearly established (25). Furthermore, changes in the stability of specific maternal mRNAs are a way of removing transcripts that encode proteins nefarious for embryonic development, as suggested for the Cdc25 gene product in *Drosophila* (7).

In *Xenopus laevis*, members of the family of maternal mRNAs, denoted Eg mRNAs, were originally identified as mRNAs that were deadenylated and released from polysomes after fertilization (17, 18). Two of these mRNAs encode proteins implicated in cell cycle control: Eg1-cdk2 (16) and Eg5, a kinesin-related protein (12). Sequence analysis suggests that the Eg2 mRNA encodes a Ser-Thr protein kinase (20a). The maternal Eg mRNAs, in addition to their postfertilization deadenylation, also undergo characteristic changes in their stability during early development. These mRNAs appear to accumulate as poly(A)$^-$ transcripts before being degraded (17). The decay of these mRNAs becomes apparent during the midblastula transition (MBT) (6).

In somatic cells, mRNA degradation can be triggered by several different mechanisms, which include poly(A) shortening, translational arrest by premature nonsense codons, and endonucleolytic cleavage (see references 5 and 22 for reviews). Each of these events requires specific sequence elements in the target mRNA.

* Corresponding author. Phone: (33) 02 99 28 61 15. Fax: (33) 02 99 28 16 49.

It follows, therefore, that the apparent temporal uncoupling between deadenylation and degradation for the Eg mRNAs could be the consequence of a functional uncoupling between these two processes. For instance, deadenylation and degradation could require different *cis*-acting sequence elements. The delayed degradation of Eg mRNAs would then be triggered by a *cis*-acting instability element recognized by a specificity factor absent or inactive in early embryos. Alternatively, deadenylation could be sufficient to trigger degradation, but at least one component of the decay pathway may be absent or limiting during the early cleavage stages. The experiments described here were undertaken to distinguish between these two hypotheses.

In a previous study (3) we showed, by injecting plasmids that directed the in vivo expression of chimeric genes, that the last 800 nucleotides (nt) of Eg2 mRNA was sufficient to prevent the accumulation of the chimeric RNA encoding the chloramphenicol acetyltransferase (CAT) reporter protein. An initial mapping experiment, which used similarly constructed chimeric genes, suggested that the sequence information responsible for this instability was located in a region consisting of the last 230 nt of Eg2-coding sequence and the first 260 nt of the 3′ untranslated region (3′UTR). Since instability motifs have been found in both coding sequences and 3′UTRs (5, 20, 22, 23), it is possible that in these chimeric RNAs, the CAT stop codon plays the role of an upstream nonsense codon relative to the 230 nt of Eg2-coding sequence. RNA decay mediated by upstream nonsense codons has been shown to occur in *X. laevis* embryos (26). Hence, the instability of these chimeric RNAs may have been a composite of several independent *cis*-acting elements.

In the present study we have focused on the 3′UTR of Eg2 mRNA so as to determine what sequence information in this region is required for the post-MBT degradation of this RNA.

This has been directly measured by monitoring the fate of RNAs injected into two-cell embryos.

## MATERIALS AND METHODS

**Plasmid constructions.** For the chimeric genes constructed in this study which contain a portion of the Eg2 3′UTR, the limits of this portion are indicated by two numbers. These correspond to the number of bases from the first nucleotide of the stop codon that terminates the Eg2 reading frame.

pGbEg2(13-667) was derived from the pGb-Eg2-800-A65 construction (11) by deleting the *Bgl*II-*Bsu*36I fragment. It contains all but the first 12 nt of the Eg2 3′UTR cloned between the cDNA of the β-globin 5′UTR and a poly(A) tail of 65 A's. The *Bgl*II site is conserved (Fig. 1).

pGbEg2(13-667) was digested with *Bsm*I, blunt ended, and then digested with *Bgl*II. The smaller *Bgl*II-*Bsm*I fragment was purified and cloned between the *Bgl*II site and the Klenow-treated *Xba*I site of pGbEg2-497 (2). This generated pGbEg2(13-414). The plasmid from which the *Bgl*II-*Bsm*I fragment had been deleted was blunt ended and recircularized. This generated pGbEg2(417-667). All of these constructions had the same general structure: a T7 promoter followed by the 5′UTR of β-globin, a fragment of the Eg2 3′UTR, the Eg2 polyadenylation signal (AATAAA), and a poly(A) tail of 65 A's, as shown in Fig. 1B.

pBSGbORF was constructed as follows. pSP64 βXm (9) was digested with *Hin*dIII and *Bsm*FI and blunt ended. This fragment, which contained the portion of β-globin cDNA consisting of the 5′UTR, the entire coding sequence (open reading frame [ORF]), and the first 70 nt of the 3′UTR, was inserted between the *Sma*I site and the blunt-ended *Sal*I site of pBS(SK$^-$) (Stratagene). In addition, the *Bam*HI site in the β-globin ORF of this plasmid was muted to *Sal*I to allow the chimeric genes to be linearized with *Bam*HI. This mutation does not change the reading frame.

pGbORF was constructed as follows. A PCR product was generated from pBSGbORF containing the *Hin*dIII site reconstituted with the 5′ PCR primer, all of the 5′UTR, the ORF, and 20 nt of the β-globin 3′UTR, followed by an *Xba*I site introduced by the 3′ PCR primer. This product was digested with *Hin*dIII, blunt ended, digested with *Xba*I, and cloned between the *Sma*I and the *Xba*I sites of BSDP1400H$^-$A65 (2).

The psGb/B4 construction (19) was used to generate an *Hin*dIII-*Pvu*II fragment corresponding to the B4 cytoplasmic polyadenylation element (CPE) and the B4 polyadenylation signal followed by a *Bam*HI site and vector sequences. This fragment was blunt ended and inserted in the blunt-ended *Hin*dIII site of pBSGbORF to generate pGbORF/B4. The chimeric gene pGbORF/B4-M6 containing the mutated CPE (B4-M6) was made similarly by using the psGb/B4-M6 construction (19).

The pGbCAT gene was constructed as follows. pSP64CAT (10) was first digested with *Bam*HI, blunt ended, and then digested with *Hin*dIII. The *Hin*dIII-*Bam*HI fragment, which contains the CAT-coding region, was purified and cloned between the *Hin*dIII and *Eco*RV sites of pSP72 (Promega) to generate pSP72CAT. pSP72CAT was digested with *Hin*dIII, blunt ended, and recircularized in the presence of *Bam*HI linkers. This plasmid was digested with *Bgl*II, blunt ended, and then digested with *Bam*HI. The *Bam*HI-*Bgl*II fragment containing the CAT-coding region was purified and cloned between the *Bgl*II site and the Klenow-treated *Xba*I site of pGbEg2-497 (2). The structures of these chimeric genes containing the globin and CAT ORF are shown in Fig. 1C.

**RNA synthesis.** $^{32}$P-labeled and capped transcripts were made in vitro by using the Promega kit as previously described (10). Poly(A)$^-$ or poly(A)$^+$ RNA was made by linearizing the plasmid with *Bam*HI or *Eco*RV, respectively, and transcribing from the T7 promoter of the Bluescribe-based vector. The transcripts were purified by electrophoresis on 5% denaturing polyacrylamide–urea gels. After visualization by autoradiography, the gel slice containing the RNA was cut out, crushed in 250 μl of extraction buffer (0.5 M NaCl, 10 mM Tris-HCl [pH 7.5], 10 mM EDTA, 1% [vol/vol] phenol-$CHCl_3$) and incubated overnight at 33°C. The acrylamide was pelleted by centrifugation (12,000 × *g*, 2 min). The supernatant was filtered by centrifugation (4,000 × *g*, 10 min) through a cellulose-acetate filter (0.22-μm pore size), extracted with 1 volume of phenol-chloroform, and precipitated with 3 volumes of 100% ethanol and 1 volume of 5 M ammonium acetate. The RNA pellet was washed twice with 70% ethanol, dried, and resuspended in water at a final concentration of 50,000 cpm/μl, corresponding to about 7.5 to 15 fmol/μl, depending on the transcript.

**Biological methods.** Eggs were obtained and fertilized by standard procedures as described by Paris et al. (17). Embryos were dejellied and injected at the two-cell stage with 18.4 nl of in vitro transcript (50,000 cpm/μl; 7.5 to 15 fmol/μl) as described by Legagneux et al. (10). Embryos were allowed to develop at 22°C.

**Analytical methods.** For each time point, the RNA from five injected embryos was extracted as described by Harland and Misher (8). Samples were diluted in 50% formamide. In all of the experiments, half of the sample was analyzed by electrophoresis on a 5% polyacrylamide–urea gel followed by autoradiography. These gels were not used for quantification, since lane-to-lane differences in signal intensity are due to variability in gel loading. RNA size markers were synthesized in vitro by using the Bluescript-based plasmid containing the phosphatase 2A cDNA linearized with different restriction enzymes (1). The other half of the RNA sample was electrophoresed on a 1% denaturing agarose gel containing 2.2 M formaldehyde and transferred onto a nylon membrane (Hybond N; Amersham) as previously described (6). The maternal ornithine decarboxylase (ODC) mRNA (1a) and the zygotic DG42 mRNA (21) were revealed by hybridizing the membranes with $^{32}$P-labeled cDNA probes as described by Duval et al. (6) except that dextran sulfate was replaced by 10% polyethylene glycol (average molecular weight, 8,000). The radioactive signals were quantified with an Instant-Imager (Packard) and the associated software (Packard Imager for Windows V 1.05). For oligo(dT)-directed RNase H digestion, the RNA extracted from five embryos was resuspended in water and treated as described previously (15).

## RESULTS

**Stability characteristics of chimeric RNAs containing portions of the Eg2 3′UTR.** To determine whether the 3′UTR of Eg2 mRNA contained sequence information sufficient to confer instability on a synthetic RNA, three chimeric genes were constructed: pGbEg2(13-667), pGbEg2(13-414), and pGbEg2 (417-667). All of these genes are terminated by a 65-A track. The structures of these chimeric genes are shown in Fig. 1B.

The RNAs corresponding to these genes were synthesized in vitro as capped $^{32}$P-labeled poly(A)$^+$ transcripts and injected into two-cell embryos. Samples of five embryos were taken for RNA extraction at various times after injection. The sequence information required for the postfertilization deadenylation of Eg2 mRNAs is contained within the distal 200 nt of the Eg2 3′UTR (2). Hence, when injected as poly(A)$^+$ transcripts, the GbEg2(13-667) and the GbEg2(417-667) RNAs should be shortened due to deadenylation. This was confirmed by analyzing these transcripts after injection into two-cell embryos (Fig. 2). The GbEg2(13-667) and GbEg2(417-667) RNAs both show the characteristic shortening that is due to sequence-specific deadenylation (2, 11). As expected, the polyadenylated GbEg2(13-414) RNA did not undergo any major change in size. Several hours after injection, the size distribution of these transcripts had become more dispersed with a slight decrease in size, characteristic of default deadenylation (10, 11), but no accumulation of the poly(A)$^-$ form was observed even during the prolonged period of this experiment.

The stabilities of these transcripts in *X. laevis* embryos were analyzed by electrophoresis of the different RNA samples in 1% agarose–formaldehyde gels followed by capillary transfer to a nylon membrane. Figure 3A shows the autoradiographic data from an experiment in which the GbEg2(13-667) RNA was coinjected with either the GbEg2(13-414) or GbEg2(417-667) RNA. In addition, the maternal Eg2 mRNA was revealed with a $^{32}$P-labeled cDNA probe, and sample recovery was checked by hybridizing the membrane with a cDNA probe to the maternal ODC mRNA. This mRNA is stable from fertilization to at least 3 h after the MBT (6). The changes in the amounts of these various RNAs were quantified by directly measuring the radioactive signals with an Instant-Imager (Packard). The data given in Fig. 3B shows that after injection, the amounts of GbEg2(13-667) and GbEg2(417-667) RNAs did not change significantly for the first 4 h (6 h postfertilization) but thereafter, a clear decrease of these RNAs was observed. Comparison of the data for the injected GbEg2(13-667) and GbEg2(417-667) RNAs with that for the maternal Eg2 mRNA showed that the instability characteristics of these injected RNAs were very similar to those of the maternal mRNA. The polyadenylated GbEg2(13-414) RNA, however, showed a remarkably greater stability. Hence, the last 250 nt of the 3′UTR of Eg2 mRNA appears to contain all of the sequence information necessary to confer a temporal change on the stability of a chimeric RNA, similar to that observed for the maternal Eg2 mRNA.

Comparable results were obtained in three other experiments. The data from these four experiments was used to calculate the half-lives ($t_{1/2}$s) of these RNAs in mid- and late

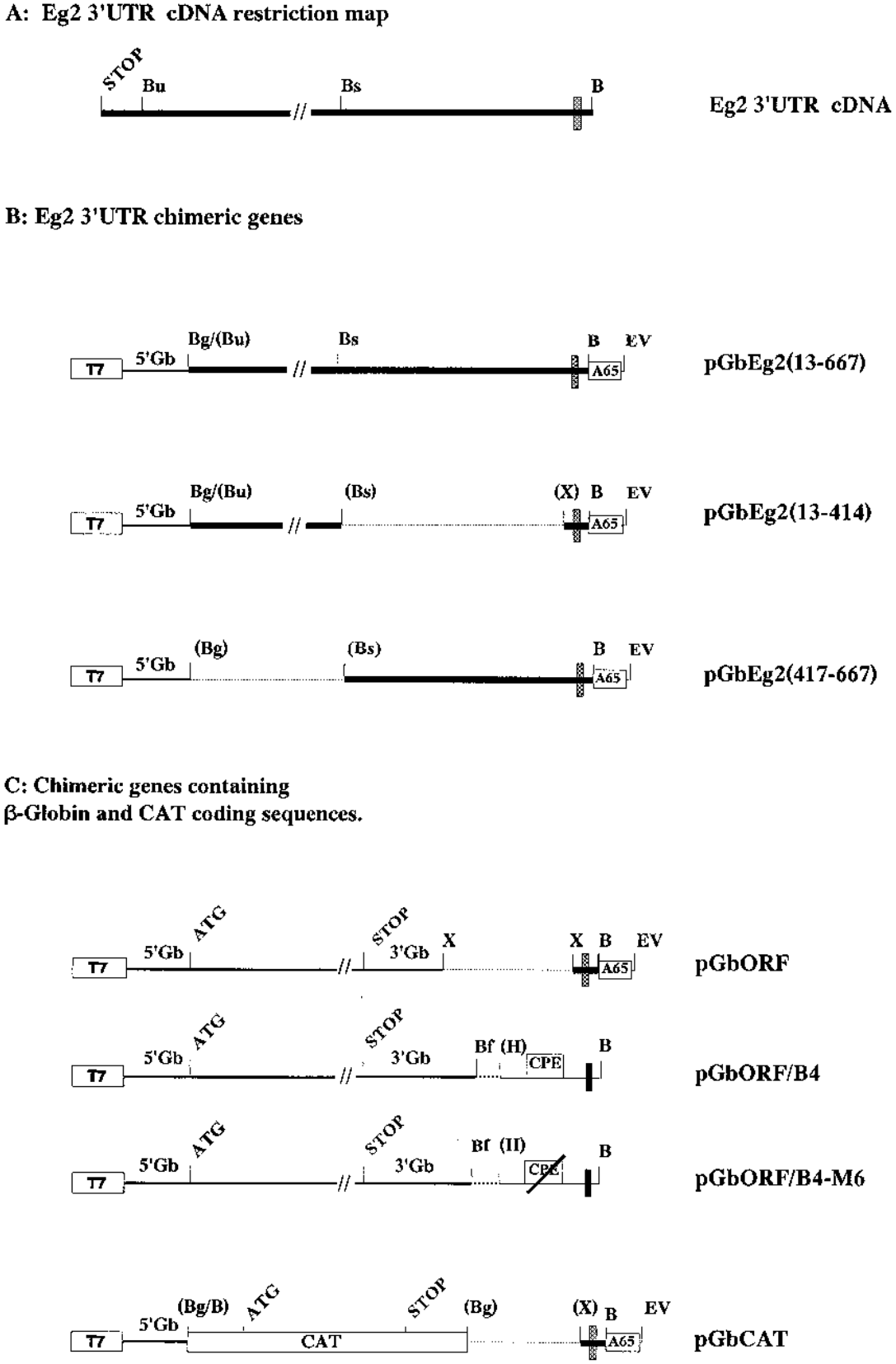


FIG. 1. Schematic diagrams of the different chimeric genes used. The names of the genes are indicated on the right. (A) Partial restriction map of the cDNA corresponding to the Eg2 3′UTR. (B) Chimeric genes derived from the Eg2 3′UTR cDNA. (C) Chimeric genes derived from the *X. laevis* β-globin, the CAT, and the *X. laevis* maternal B4 cDNAs. Translation initiation (ATG) and termination (STOP) codons are indicated. 5′Gb and 3′Gb, 5′UTR and 3′UTR of β-globin mRNA, respectively. Boxes represent the positions of the T7 promoter, the CAT sequence, the B4 CPE, and the track of 65 A's, as denoted. The CPE box with a diagonal bar denotes the nonfunctional CPE mutant. Heavy lines, portions of the Eg2 cDNA; medium lines, portions of the β-globin cDNA; thin lines, portions of B4 cDNA sequence. Hatched box, Eg2 polyadenylation signal; black box, B4 polyadenylation signal. Lines of thin dots, deletions; lines of heavy dots, plasmid sequence. Restriction sites: B, *Bam*HI; Bf, *Bsm*FI; Bg, *Bgl*II; Bs, *Bsm*I; Bu, *Bsu*36I; EV, *Eco*RV; H, *Hin*dIII; X, *Xba*I. Restriction sites between brackets indicate sites lost during cloning.

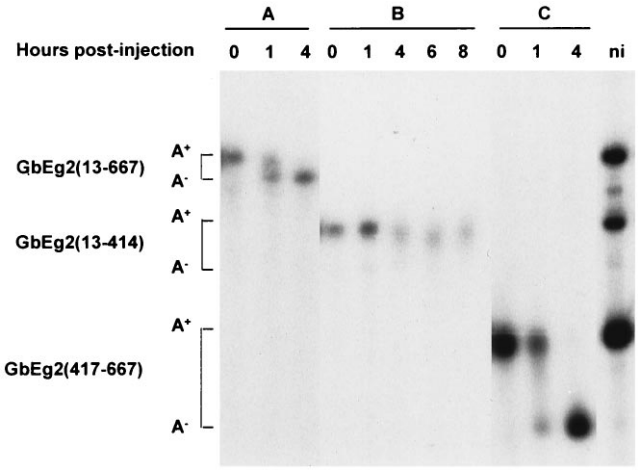


FIG. 2. Deadenylation of the chimeric GbEg2 RNA injected into two-cell embryos. Between 0.15 and 0.3 fmol of the different $^{32}$P-labeled and capped Eg2 chimeric RNAs was injected as polyadenylated ($A^+$) RNAs into two-cell embryos, as described in Materials and Methods. Samples of five embryos were taken for RNA extraction at the indicated times after injection, and aliquots corresponding to 2.5 embryo equivalents were analyzed on a 5% polyacrylamide–urea gels. After drying, the gel was subjected to autoradiography. ni, noninjected mixture of these RNAs. The sizes of these poly(A)$^+$ RNAs are as follows: GbEg2(13-667), 828 nt; GbEg2(13-414), 607 nt; GbEg2(417-667), 429 nt. The positions of the poly(A)$^+$ and poly(A)$^-$ forms of these RNAs are indicated on the left. A, GbEg2(13-667); B, GbEg2(13-414); C, GbEg2(417-667).

blastula stage embryos: maternal Eg2 mRNA, 3.9 ± 1.1 h; GbEg2(13-667) and GbEg2(417-667) RNAs, 3.8 ± 0.9 h; and GbEg2(13-414) and ODC, RNAs ≥20 h (see Fig. 6).

**Stability characteristics of poly(A)$^+$ and poly(A)$^-$ globin RNAs.** The results described above show that the same region of the Eg2 3′UTR that confers deadenylation on an RNA was also required for the subsequent degradation of these RNAs. This opens the possibility that the degradation of these mRNAs at the blastula stage could be a direct consequence of their prior deadenylation. This would imply that no additional *cis*-acting instability element(s) is required to trigger the degradation of Eg mRNAs. We reasoned that it would be possible to verify this hypothesis by analyzing the stability characteristics of chimeric RNAs that are devoid of *cis*-acting sequence information that controls adenylation.

Chimeric genes were therefore constructed that contained all of the 5′UTR and the coding sequence of *X. laevis* β-globin and in which the 3′UTR was composed of the first 20 nt of the β-globin 3′UTR followed by the polyadenylation signal and the 65-nt poly(A) track present in the chimeric RNAs used previously (Fig. 1C). The corresponding RNAs were synthesized as capped $^{32}$P-labeled transcripts in a poly(A)$^+$ or a poly(A)$^-$ form. These RNAs were injected into two-cell embryos, and samples of five embryos were taken for RNA extraction at various times. The polyadenylation status of these two transcripts was verified by electrophoresis of aliquots on a polyacrylamide-urea gel. The data given in Fig. 4A shows that after injection, the poly(A)$^+$ GbORF RNA slightly decreased in size in a manner indicative of default deadenylation (11). That the vast majority of these RNAs remain adenylated was confirmed by oligo(dT)-directed RNase H treatment of the 8-h sample (Fig. 4B). The poly(A)$^-$ GbORF RNA did not change in size throughout the whole experiment. Essentially identical results were obtained in all of the experiments performed with the GbORF RNAs. The stability characteristics of these two RNAs were analyzed by electrophoresis in 1% agarose–formaldehyde gels followed by transfer to nylon membranes. The autoradiograms for two different experiments are shown in Fig. 4C. In both experiments the MBT, detected by the presence of the zygotic transcript DG42, occurred at about 6 h of development. Sample recovery was verified by hybridizing the membrane with a $^{32}$P-labeled cDNA probe to ODC maternal mRNA. From both of these sets of autoradiograms it is clear that the poly(A)$^+$ GbORF RNA is more stable than the poly(A)$^-$ counterpart. Quantitative data for the stabilities of these RNAs and for the recovery of the maternal ODC mRNA was obtained by using an Instant-Imager (Fig. 4D). Results from experiments in which the signal for ODC mRNA fluctuated by more than 10% from the average value were not retained for further analysis. This quantitative data confirmed that the poly(A)$^+$ GbORF RNA was quasistable throughout the period studied. However, in the five experiments performed with the poly(A)$^+$ and poly(A)$^-$ GbORF RNAs, a variability was observed in the time at which the degradation of the poly(A)$^-$ GbORF was initiated. The two experiments shown in Fig. 4C and D represent the extreme cases. In the experiment shown in the right panels, poly(A)$^-$ GbORF RNA was initially almost as stable as its poly(A)$^+$ counterpart and then started to decrease in amount after about 6 h postinjection (8 h of development). For the experiment shown in the left panels, no delay in the degradation of the poly(A)$^-$ GbORF RNA was observed. Despite this difference, in all of the experiments the poly(A)$^-$ GbORF RNA was always degraded, whereas the poly(A)$^+$ GbORF RNA was essentially stable. The data from five experiments was used to calculate the average $t_{1/2}$ of the GbORF RNA in *X. laevis* embryos. For the transcripts injected in a poly(A)$^+$ form, data from the whole period studied was used for this calculation, which gave a $t_{1/2}$ of ≥20 h. For the transcripts injected in a poly(A)$^-$ form, the $t_{1/2}$ was calculated for the period after the 6-h-postinjection time point, when degradation of these RNAs was always observed. This yielded a $t_{1/2}$ of 4.8 ± 1.5 h. This value for the poly(A)$^-$ GbORF RNA is comparable to that for the maternal Eg2 mRNA and the GbEg2(13-667) and GbEg2(417-667) chimeric RNAs that are deadenylated after injection (see Fig. 6).

**Stability characteristics of poly(A)$^+$ and poly(A)$^-$ GbCAT RNAs.** To confirm that this differential stability of the poly(A)$^+$ and poly(A)$^-$ GbORF RNAs was not specific to this reporter gene, similar experiments were performed with poly(A)$^+$ and poly(A)$^-$ GbCAT RNAs. In these RNAs, which have the same general structure as the GbORF RNAs, the globin-coding region was replaced by the coding region for the CAT protein (Fig. 1C). Representative autoradiograms obtained from the analysis of these RNAs by electrophoresis in agarose-formaldehyde gels are shown in Fig. 5A. As described above, hybridizing the membrane with the appropriate $^{32}$P-labeled cDNA probes allowed the MBT to be situated and sample recovery to be verified. Instant-Imager quantification showed that the injected poly(A)$^+$ GbCAT RNA was more stable than the injected poly(A)$^-$ GbCAT RNA (Fig. 5B). Polyacrylamide-urea gel electrophoretic analysis did not detect any significant change in the size of these RNAs (data not shown). This was confirmed by oligo(dT)-directed RNase H digestion of the 8-h-postinjection sample (Fig. 5C). The data from four experiments was used to calculate the average $t_{1/2}$s of the poly(A)$^+$ and poly(A)$^-$ GbCAT RNAs in *X. laevis* embryos: poly(A)$^+$ GbCAT, 11.8 ± 2.4 h, and poly(A)$^-$ GbCAT, 5.9 ± 1.2 h (see Fig. 6). Since no delay in the degradation of this poly(A)$^-$ RNA was observed, these values were calculated for the entire period studied. The data summarized in Fig. 6 show that the poly(A)$^+$ GbCAT RNA was not as stable as the poly(A)$^+$ GbORF RNA. This lesser stability of the injected

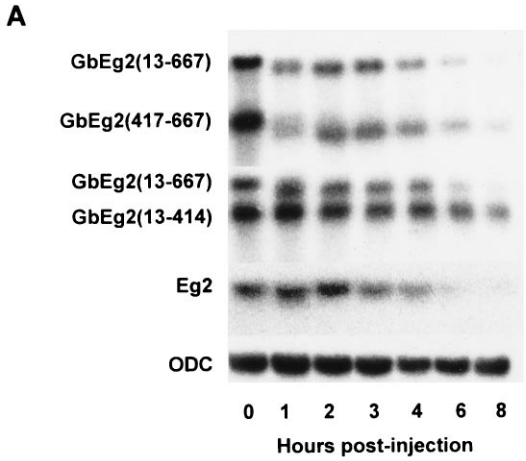


FIG. 3. Comparison of the stabilities of the chimeric GbEg2 RNAs and of the maternal Eg2 and ODC mRNAs. Two-cell embryos were injected with $^{32}$P-labeled, capped, and polyadenylated RNAs. Samples of five embryos were taken for RNA extraction at the indicated times after injection, and aliquots corresponding to 2.5 embryo equivalents were analyzed on a denaturing agarose gel (1%) and transferred to a nylon membrane. This membrane was autoradiographed and quantified with an Instant-Imager. The maternal ODC and Eg2 mRNAs were then revealed with the appropriate $^{32}$P-labeled cDNA probes, and the membrane was autoradiographed and quantified as described above. (A) Analysis of the injected $^{32}$P-labeled transcripts and of the maternal Eg2 and ODC mRNAs. GbEg2(13-667) RNA was coinjected with either the GbEg2(13-414) RNA or the GbEg2(417-667) RNA, as indicated on the left. (B) Graphical representation of the data obtained by Instant-Imager quantification of the experiments shown in panel A. The values at the different time points are expressed as percentages of RNA remaining. (Top) Data for the maternal Eg2 and ODC mRNAs. (Bottom) Data for the injected chimeric GbEg2 RNAs.

poly(A)$^+$ GbCAT RNA relative to that of the poly(A)$^+$ GbORF RNA is not due to a precocious deadenylation of the GbCAT RNA (Fig. 5C). Rather, the reduced stability of the poly(A)$^+$ GbCAT RNA appears to be a characteristic of this reporter gene.

**CPE-driven polyadenylation protects injected RNAs from degradation.** A consequence of the results summarized in Fig. 6 is that if a poly(A)$^-$ transcript were to be adenylated after injection, it should be protected from being degraded. To test this, a chimeric gene was constructed that contained all of the 5′UTR and the coding sequence of the *X. laevis* β-globin and in which the 3′UTR was composed of the first 70 nt of the β-globin 3′UTR followed by the *X. laevis* B4 CPE and the polyadenylation signal (GbORF/B4) (Fig. 1C). As a control a chimeric gene was also made by using a mutant (nonfunctional) form of the B4-CPE (B4-M6) (GbORF/B4-M6) (19). The RNAs corresponding to these genes were synthesized as capped $^{32}$P-labeled poly(A)$^-$ transcripts and injected into two-cell embryos. After injection, samples of five embryos were taken, and RNA was extracted and analyzed for changes in both adenylation and stability.

The changes in the polyadenylation status of these two RNAs was verified by electrophoresis in polyacrylamide-urea gels (Fig. 7A). As expected, the GbORF/B4 mRNA rapidly increased in size after injection. This RNA attained a length about 100 nt longer than that of the in vitro-synthesized poly(A)$^-$ transcript. The GbORF/B4-M6 RNA showed no significant change in size throughout the duration of the experiment. Chromatography of the 0- and 8-h samples on poly(rU) agarose columns confirmed that the size increase for the GbORF/B4 RNA in the 8-h sample was due to polyadenylation; the GbORF/B4-M6 RNA in the 8-h samples was not retained on the poly(rU) agarose column (data not shown).

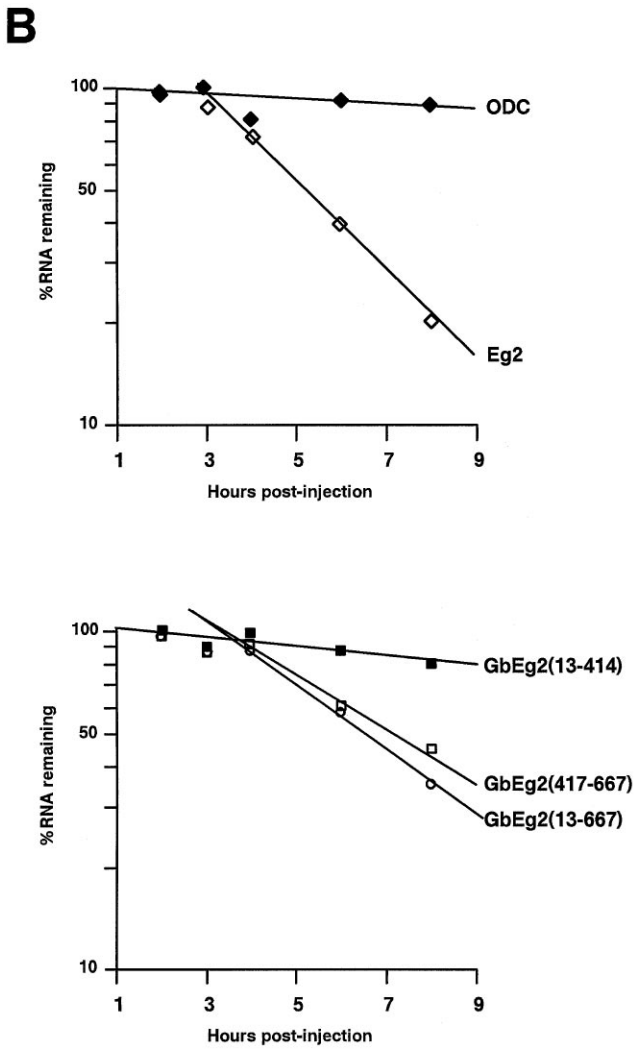


The stability characteristics of these two RNAs were analyzed by electrophoresis in a 1% agarose–formaldehyde gel followed by transfer to a nylon membrane and autoradiography (Fig. 7B). As described for the previous experiments, hybridization of the membrane with the appropriate $^{32}$P-labeled cDNA probes allowed the MBT to be situated and sample recovery to be verified. The quantification (Instant-Imager) of this experiment (Fig. 7C) showed that the GbORF/B4 RNA did not change in stability throughout the entire experiment. The amount of this RNA decreased slightly, with a $t_{1/2}$ of about 20 h. In contrast, the GbORF/B4-M6 RNA clearly started to decrease in amount after 6 h postinjection, with a $t_{1/2}$ of about 3 h. Therefore, the in vivo adenylation of the GbORF/B4 RNA, which was injected in a poly(A)$^-$ form, protected the RNA from degradation.

## DISCUSSION

Previous work from this laboratory has shown that although the deadenylation of the maternal *X. laevis* Eg mRNAs is initiated at or soon after fertilization, no decrease in their total amount was detected before the MBT (6, 17). One possible hypothesis to account for this temporal separation between deadenylation and degradation was that of completely inde-

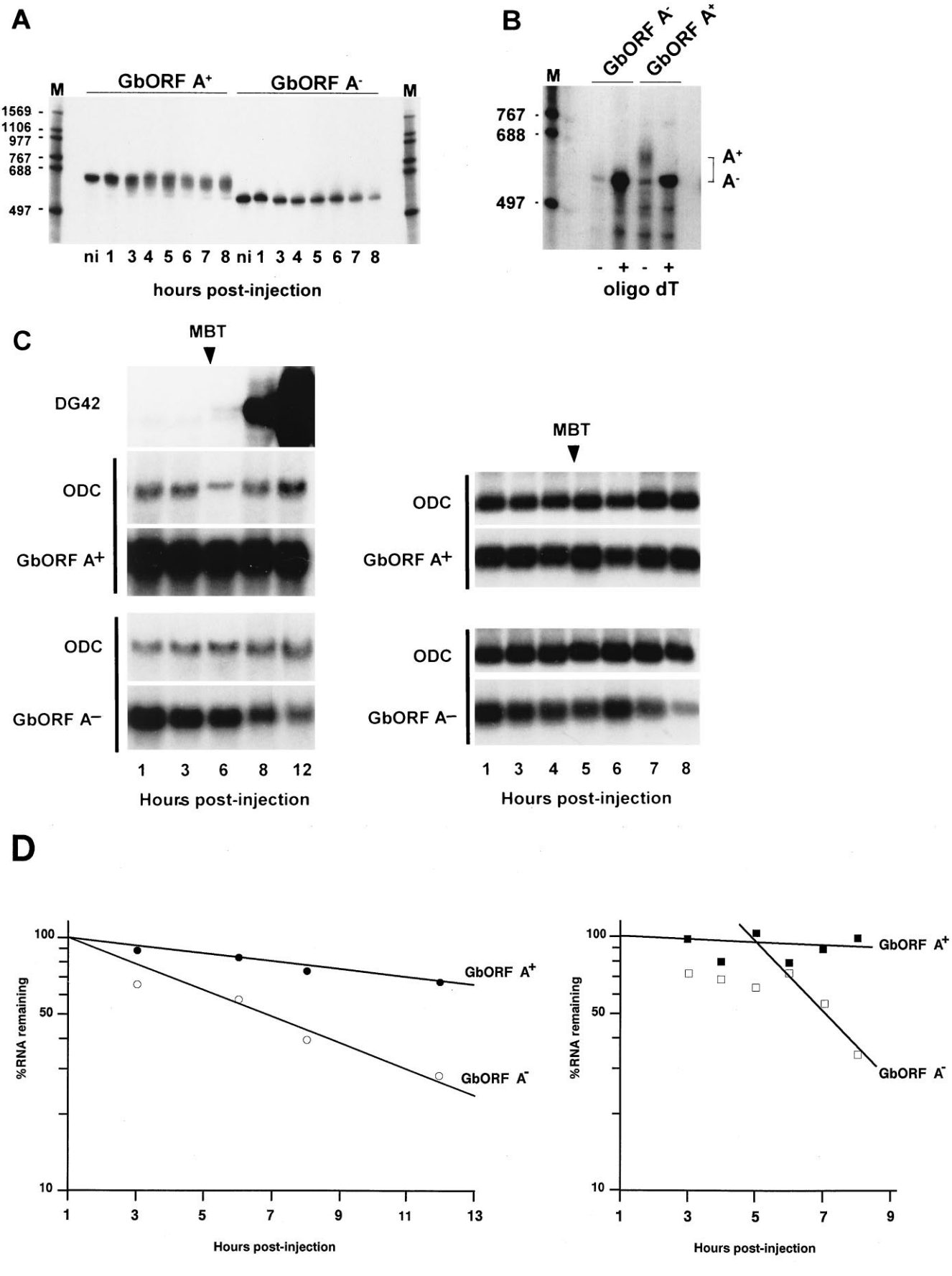
A
M
GbORF A+
GbORF A-
M
1569
1106
977
767
688
497
ni 1 3 4 5 6 7 8 ni 1 3 4 5 6 7 8
hours post-injection
B
GbORF A-
GbORF A+
M
767
688
497
A+
A-
- + - +
oligo dT
C
MBT
DG42
ODC
GbORF A+
ODC
GbORF A–
1 3 6 8 12
Hours post-injection
MBT
ODC
GbORF A+
ODC
GbORF A–
1 3 4 5 6 7 8
Hours post-injection
D
100
50
10
%RNA remaining
GbORF A+
GbORF A-
1 3 5 7 9 11 13
Hours post-injection
100
50
10
%RNA remaining
GbORF A+
GbORF A-
1 3 5 7 9
Hours post-injection

FIG. 4. Analysis of the adenylation-deadenylation and stability behaviors of the injected poly(A)$^+$ and poly(A)$^-$ GbORF RNAs. The indicated $^{32}$P-labeled RNAs were injected as described in the legend to Fig. 2. Sample of five embryos were taken at the indicated times after injection, and the eventual changes in sizes were analyzed on 5% polyacrylamide–urea gels as described in the legend to Fig. 2 or by oligo(dT)-directed RNase H treatment of the 8-h samples. Changes in stability were analyzed as described in the legend to Fig. 3. (A) Analysis of the sizes of the injected RNAs. On the left is shown the data for the injected poly(A)$^+$ GbORF RNA. On the right is shown the poly(A)$^-$ counterpart. Lanes M, RNA molecular weight markers. The lanes ni, corresponding noninjected RNAs. (B) Oligo(dT)-directed RNase H analysis of the injected poly(A)$^+$ and poly(A)$^-$ GbORF. The 8-h samples were treated with RNase H in the absence (−) or presence (+) of oligo(dT). Lanes M, RNA molecular weight markers. On the right are indicated the positions of the poly(A)$^+$ and poly(A)$^-$ GbORF RNAs. (C) Analysis of the stabilities of the injected poly(A)$^+$ and poly(A)$^-$ GbORF RNAs in two different sets of experiments. The maternal ODC mRNA was visualized to control for the efficiency of RNA extraction. The MBT was situated relative to the signal for the zygotic DG42 mRNA. (D) Quantification of the injected RNAs. The data are expressed as described in the legend to Fig. 3B. Closed symbols correspond to injected poly(A)$^+$ RNA, and open symbols correspond to injected poly(A)$^-$ RNA. The circles correspond to the GbORF data for Fig. 4C, left panel, and the squares correspond to the GbORF data for Fig. 4C, right panel.

pendent pathways targeted by distinct *cis*-acting elements. Alternatively, the degradation of Eg RNAs may be triggered by deadenylation, with the delay in degradation being caused, for instance, by a limiting amount of a component in this pathway (see the introduction). In the present study we showed that when the sequence information from the Eg2 mRNA was restricted to that of the 3′UTR, only those chimeric RNAs that were deadenylated were also degraded. Next we showed that the poly(A)$^-$ form of RNAs containing either the globin or the CAT coding sequence, and devoid of a CPE or a deadenylation

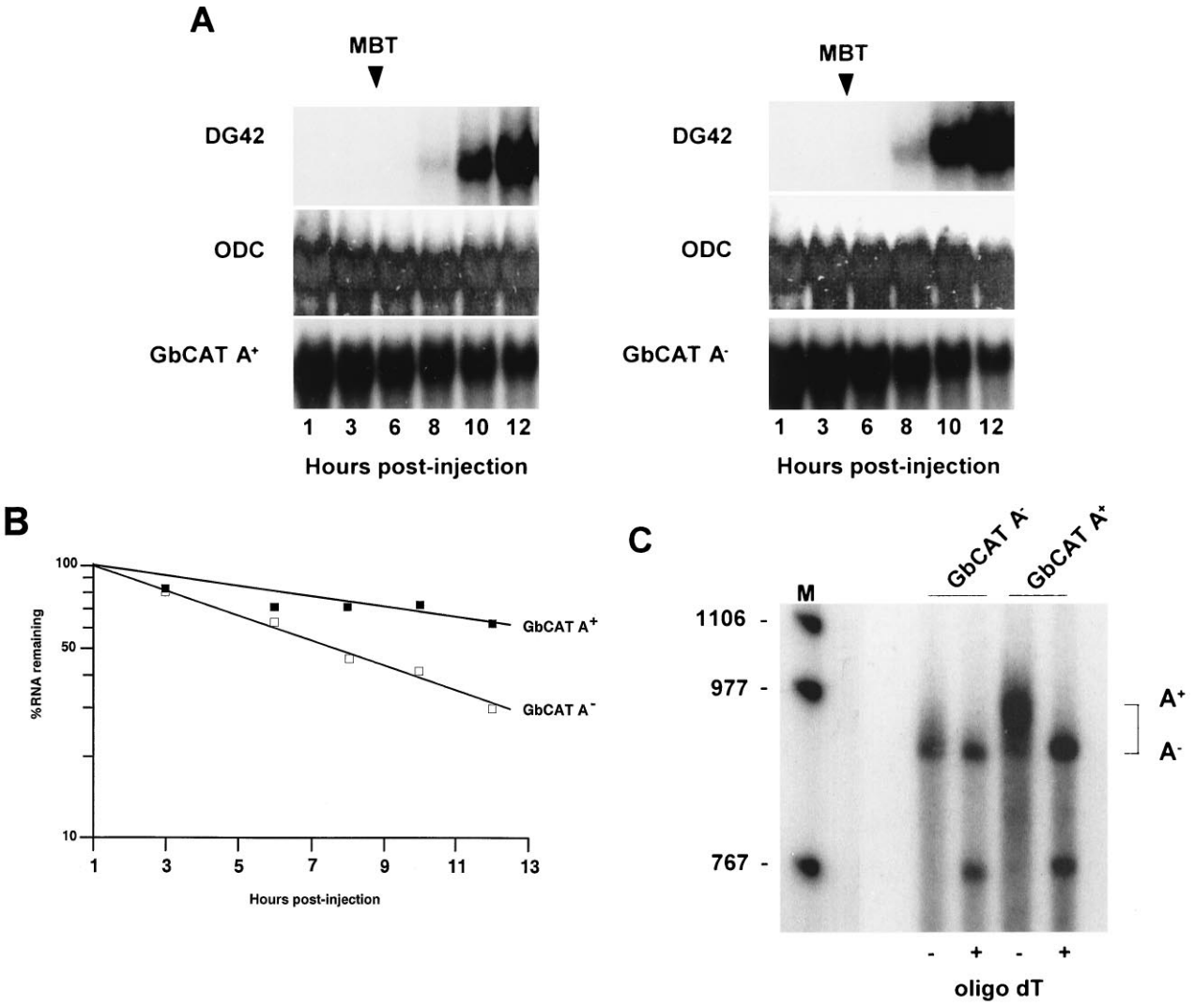


FIG. 5. Analysis of the stability and the adenylation-deadenylation behaviors of the injected poly(A)$^+$ and poly(A)$^-$ GbCAT RNAs. The indicated $^{32}$P-labeled chimeric RNAs were injected and analyzed as described in the legends to Fig. 2 and 3. (A) Analysis of the stabilities of the injected poly(A)$^+$ and poly(A)$^-$ GbCAT RNAs on formaldehyde-agarose gels. The maternal ODC mRNA was visualized to control for the efficiency of RNA extraction. The MBT was situated relative to the signal for the zygotic DG42 mRNA. (B) Quantification of the injected RNAs. The data are expressed as described in the legend to Fig. 3B. Symbols: ■, injected poly(A)$^+$ GbCAT RNA; □, injected poly(A)$^-$ GbCAT RNA. (C) Oligo(dT)-directed RNase H analysis of the injected poly(A)$^+$ and poly(A)$^-$ GbORF RNAs. The 8-h RNA samples were treated with RNase H in the absence (−) or presence (+) of oligo(dT). Lanes M, RNA molecular weight markers. On the right the positions of the poly(A)$^+$ and poly(A)$^-$ GbCAT RNAs are indicated.

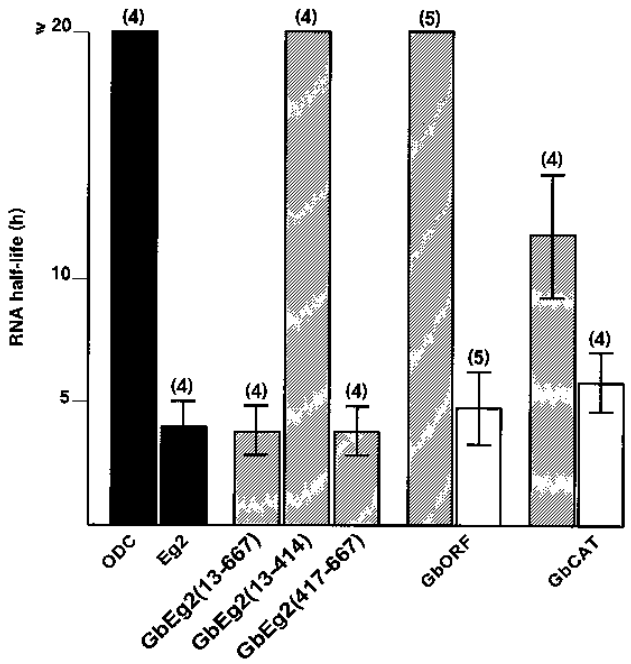


FIG. 6. Comparison of the $t_{1/2}$s of the injected and maternal RNAs. Values are given as averages ± standard deviations calculated from the number of experiments indicated above each bar. Black bars, maternal mRNAs; hatched bars, injected poly(A)$^+$ RNAs; open bars, injected poly(A)$^-$ RNAs.

element, was degraded at a rate similar to that of the maternal Eg2 mRNA or the deadenylated chimeric RNAs derived from this maternal transcript. Last, we showed that an RNA injected as a poly(A)$^-$ transcript was protected from degradation by in vivo polyadenylation. We conclude, therefore, that deadenylation is sufficient to cause the degradation of an mRNA in blastula stage embryos and that the degradation of the Eg2-derived RNAs does not require any specific sequence information, other than that necessary to achieve deadenylation.

Harland and Misher (8) have shown previously that RNAs encoding the CAT protein were degraded in *X. laevis* embryos. Over the 27-h period studied, the nonadenylated CAT RNA was degraded with a $t_{1/2}$ of 3 to 4 h, and the CAT and human globin RNAs with poly(A) tails of 80 and 60 nt, respectively, were degraded as rapidly as the nonadenylated CAT transcripts. This is at variance with the results presented here, where a poly(A) tail of 65 nt efficiently stabilized both β-globin and CAT RNAs (Fig. 6). Differences in the rates of default deadenylation (that which is not sequence specific) could be the cause of this apparent discrepancy.

In *X. laevis* embryos, RNAs that are devoid of both a CPE and a *cis*-acting deadenylation element, such as the GbCAT, GbORF, and GbEg2(13-414) chimeric RNAs, are still substrates for default deadenylation (reference 10 and this study). This default deadenylation, which is much slower than the Eg-specific deadenylation (11), causes the gradual decrease in size that was observed for the poly(A)$^+$ GbEg2(13-414), GbORF, and GbCAT transcripts (Fig. 2, 4, and 5). In the present study the vast majority of these RNAs remained adenylated and therefore protected from degradation. Harland and Misher (8) noted that in their experiments the adenylated CAT RNAs were initially heterogeneous in size and that they were continuously shortened until they reached the size of the poly(A)$^-$ RNA. This is indicative of a default deadenylation which was much more active than that in the experiments described here and which would render the overall rate of degradation of the RNAs injected with a poly(A) tail of 60 or 80 nt indistinguishable from that of the injected poly(A)$^-$ RNAs. Similarly, the presence of a longer poly(A) tail (200 nt) would probably only marginally increase the overall stability of the RNAs, as was observed by Harland and Misher (8). The apparent difference in the rates of default deadenylation in these two studies could be related to the way in which the embryos were allowed to develop. In the experiments described here, all of the embryos were incubated at 22°C. In the experiments performed by Harland and Misher (8), batches of the injected embryos were incubated at various temperatures between 15 and 22°C, so as to obtain, at any one time, embryos at different developmental stages. Thus, if embryonic development was slowed by the reduced temperature to a greater extent than the rate of default deadenylation, then at a particular stage of development at the low temperature, deadenylation would have proceeded further than in embryos at the same stage but incubated at 22°C.

In a previous study (3) we showed that the 490-nt portion of Eg2 mRNA that contains the last 230 nt of Eg2-coding sequence and the first 260 nt of the 3′UTR conferred instability on a chimeric RNA (named CAT-497) containing the CAT reporter gene. RNAs containing this region of Eg2 RNA are not rapidly deadenylated in *X. laevis* embryos (2, 10). Therefore, the degradation of the CAT-497 RNA presumably occurs by a deadenylation-independent mechanism. We have shown here that the poly(A)$^+$ GbEg2(13-414) RNA is not unstable, implying that the first 260 nt of the Eg2 3′UTR does not contain an instability element. Hence, the deadenylation-independent degradation of the CAT-497 RNA could be due either to an instability element in the last 230 nt of the coding region or, as mentioned in the introduction, to nonsense-mediated mRNA decay, triggered by the CAT stop codon. Work is in progress to elucidated this point.

In both yeast and mammalian cells, poly(A)$^-$ intermediates are not normally observed, which implies that the rate at which the deadenylated RNAs are produced does not exceed the capacity of the degradation machinery in these cells. In *X. laevis* embryos the situation is somewhat different, as there is a transient accumulation of poly(A)$^-$ mRNAs, presumably due to a lag between deadenylation and degradation. Several hypotheses can be formulated to explain this lag between deadenylation and degradation in *X. laevis* embryos. For instance, the capacity of the degradation machinery could be insufficient to immediately degrade all of the poly(A)$^-$ RNA produced by deadenylation. Alternatively, the poly(A)$^-$ RNA could be (or become) associated with RNA-binding proteins, thereby forming a type of storage particle in which the RNA is at least partially protected from degradation. These proteins may be related to those implicated in the storage of maternal mRNAs in oocytes (reviewed in reference 24). For yeast, decay pathways where deadenylation leads to either 5′-decapping and degradation by a 5′-3′ exoribonuclease (13) or, in some cases, to degradation by a 3′-5′ exoribonuclease (14; for a review, see reference 4) have been described. Uncapped RNAs are rapidly degraded in *X. laevis* embryos. Therefore, if the degradation of RNAs in *X. laevis* embryos was to proceed along similar pathways, the lag between deadenylation and degradation could be caused by a limiting amount of one of the components responsible for the poly(A)$^-$-dependent 5′-decapping activity. As mentioned above, protection of the RNA from the degradation machinery could also explain the lag between deadenylation and degradation. In this case it would be the dissociation (partial or total) of the storage particle that would allow degradation of the RNA.

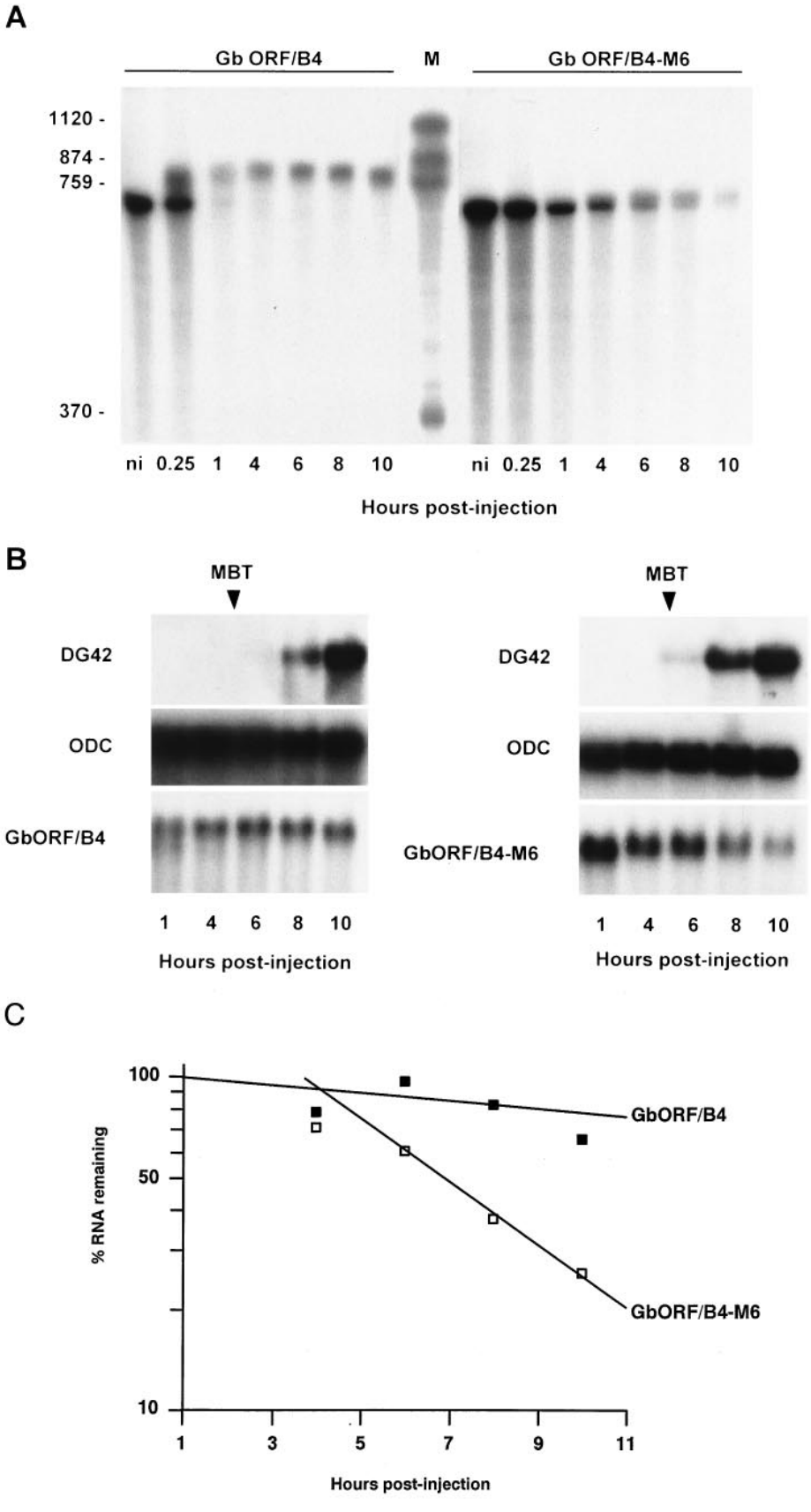


FIG. 7. Analysis of adenylation and stability behaviors of the injected poly(A)$^-$ GbORF/B4 and GbORF/B4-M6 RNAs. The indicated $^{32}$P-labeled, poly(A)$^-$ RNAs were injected and analyzed as described in the legends to Fig. 2 and 3. (A) Analysis of the sizes of the injected RNAs on 5% polyacrylamide–urea gels. Lanes M, RNA molecular weight markers. ni, noninjected RNA. (B) Analysis of the stabilities of GbORF/B4 and GbORF/B4-M6 RNAs on denaturing agarose gels with the same RNA samples as analyzed in panel A. (C) Graphical representation of the Instant-Imager quantification of the experiment shown in panel B. The data were expressed as described in the legend to Fig. 3B.

In fact, there is some circumstantial evidence to support both hypotheses, which suggests that it may well be a combination of both a limiting component and protection that is responsible for the observed delay in the degradation of the poly(A)$^-$ maternal mRNAs. In some experiments described here, the injected poly(A)$^-$ GbORF RNA was degraded continuously, whereas in others these RNAs were initially stable. It is conceivable that these different behaviors for the same transcript could be due to a batch-to-batch variations in the rate at which the injected RNA becomes protected by association with the endogenous RNA-binding proteins. For the maternal mRNAs this association with protective factors should always be effective either because it already exists or because it proceeds continuously as the poly(A) tail is shortened. Alternatively, we have shown previously that the ongoing translation of one or several maternal mRNAs appears to be required for the degradation of the maternal Eg2 mRNA (3, 6). This observation is compatible with the notion of a limiting component of the degradation machinery that is a labile protein.

## ACKNOWLEDGMENTS

We thank Vincent Legagneux for comments on the manuscript.

This work was supported by grants from the Institut National de la Santé et de la Recherche Médicale (CRE 91-0112), the European Economic Community Biotechnology Program (BIO4-CT95-0045), the Ministère Chargé de la Recherche (ACC-SV4), and the Association pour la Recherche sur le Cancer (contract 6788).

## REFERENCES

1. **Audic, Y., F. Omilli, and H. B. Osborne.** Unpublished data.
1a. **Bassez, T., J. Paris, F. Omilli, C. Dorel, and H. B. Osborne.** 1990. Post-transcriptional regulation of ornithine decarboxylase in Xenopus laevis oocytes. Development **110:**955–962.
2. **Bouvet, P., F. Omilli, Y. Arlot-Bonnemains, V. Legagneux, C. Roghi, T. Bassez, and H. B. Osborne.** 1994. The deadenylation conferred by the 3′ untranslated region of a developmentally controlled mRNA in *Xenopus* embryos is switched to polyadenylation by deletion of a short sequence element. Mol. Cell. Biol. **14:**1893–1900.
3. **Bouvet, P., J. Paris, M. Philippe, and H. B. Osborne.** 1991. Degradation of a developmentally regulated mRNA in *Xenopus* embryos is controlled by the 3′ region and requires the translation of another maternal mRNA. Mol. Cell. Biol. **11:**3115–3124.
4. **Caponigro, G., and R. Parker.** 1996. Mechanisms and control of mRNA turnover in *Saccharomyces cerevisae*. Microbiol. Rev. **60:**233–249.
5. **Decker, C. J., and R. Parker.** 1994. Mechanisms of mRNA degradation in eukaryotes. Trends Biochem. Sci. **19:**336–340.
6. **Duval, C., P. Bouvet, F. Omilli, C. Roghi, C. Dorel, R. LeGuellec, J. Paris, and H. B. Osborne.** 1990. Stability of maternal mRNA in *Xenopus* embryos: role of transcription and translation. Mol. Cell. Biol. **10:**4123–4129.
7. **Edgar, B. A., and S. A. Datar.** 1996. Zygotic degradation of two maternal Cdc25 mRNAs terminates Drosophila early cell cycle program. Genes Dev. **10:**1966–1977.
8. **Harland, R., and L. Misher.** 1988. Stability of RNA in developing Xenopus embryos and identification of a destabilizing sequence in TFIIIA messenger RNA. Development **102:**837–852.
9. **Krieg, P. A., and D. A. Melton.** 1984. Functional messenger RNAs are produced by SP6 in vitro transcription of cloned cDNA. Nucleic Acids Res. **12:**7057–7070.
10. **Legagneux, V., P. Bouvet, F. Omilli, S. Chevalier, and H. B. Osborne.** 1992. Identification of RNA-binding proteins specific to Xenopus Eg maternal mRNAs: association with the portion of Eg2 mRNA that promotes deadenylation in embryos. Development **116:**1193–1202.
11. **Legagneux, V., F. Omilli, and H. B. Osborne.** 1995. Substrate-specific regulation of RNA deadenylation in Xenopus embryo and activated egg extracts. RNA **1:**1001–1008.
12. **LeGuellec, R., J. Paris, A. Couturier, C. Roghi, and M. Philippe.** 1991. Cloning by differential screening of a *Xenopus* cDNA that encodes a kinesin-related protein. Mol. Cell. Biol. **11:**3395–3398.
13. **Muhlrad, D., C. J. Decker, and R. Parker.** 1994. Deadenylation of the unstable mRNA encoded by the yeast MFA2 gene leads to decapping followed by 5′-3′ digestion of the transcript. Genes Dev. **8:**855–866.
14. **Muhlrad, D., C. J. Decker, and R. Parker.** 1995. Turnover mechanisms of the stable yeast PGK1 mRNA. Mol. Cell. Biol. **15:**2145–2156.
15. **Osborne, H. B., C. Duval, L. Ghoda, F. Omilli, T. Bassez, and P. Coffino.** 1991. Expression and post-transcriptional regulation of ornithine decarboxylase during early Xenopus development. Eur. J. Biochem. **202:**575–581.
16. **Paris, J., R. LeGuellec, A. Couturier, K. LeGuellec, F. Omilli, J. Camonis, S. MacNeil, and M. Philippe.** 1991. Cloning by differential screening of a Xenopus cDNA coding for a protein highly homologous to cdc2. Proc. Natl. Acad. Sci. USA **88:**1039–1043.
17. **Paris, J., H. B. Osborne, A. Couturier, R. LeGuellec, and M. Philippe.** 1988. Changes in the polyadenylation of specific stable RNAs during the early development of Xenopus laevis. Gene **72:**169–176.
18. **Paris, J., and M. Philippe.** 1990. Poly(A) metabolism and polysomal recruitment of maternal mRNAs during early Xenopus development. Dev. Biol. **140:**221–224.
19. **Paris, J., K. Swenson, H. Piwnica-Worms, and J. D. Richter.** 1991. Maturation-specific polyadenylation: in vitro activation by p34cdc2 and phosphorylation of a 58-kD CPE-binding protein. Genes Dev. **5:**1697–1708.
20. **Peltz, S. W., A. H. Brown, and A. Jacobson.** 1993. mRNA destabilization triggered by premature translational termination depends on at least three cis-acting sequence elements and one trans-acting factor. Genes Dev. **7:**1737–1754.
20a. **Roghi, C.** Personal communication.
21. **Rosa, F., T. D. Sargent, M. L. Rebbert, G. S. Michaels, M. Jamrich, H. Grunz, E. Jonas, J. A. Winkles, and I. B. Dawid.** 1988. Accumulation and decay of DG42 gene products follow a gradient pattern during Xenopus embryogenesis. Dev. Biol. **129:**114–123.
22. **Sachs, A. B.** 1993. Messenger RNA degradation in eukaryotes. Cell **74:**413–421.
23. **Shyu, A. B., J. G. Belasco, and M. E. Greenberg.** 1991. Two distinct destabilizing elements in the c-fos message trigger deadenylation as a first step in rapid mRNA decay. Genes Dev. **5:**221–231.
24. **Sommerville, J.** 1992. RNA-binding proteins: masking proteins revisited. Bioessays **14:**337–339.
25. **St. Johnston, D., and C. Nüsslein-Volhard.** 1992. The origin of pattern and polarity in the Drosophila embryo. Cell **68:**201–219.
26. **Whitfield, T. T., C. R. Sharpe, and C. C. Wylie.** 1994. Nonsense-mediated mRNA decay in Xenopus oocytes and embryos. Dev. Biol. **165:**731–734.